# LONGITUDINAL SHEAR PROPERTIES OF EUROPEAN LARCH WOOD RELATED TO CELL-WALL STRUCTURE

## Ulrich Müller

Assistant Professor

## Aleksandra Sretenovic

Graduate Researcher

## Wolfgang Gindl†

Associate Professor

and

## Alfred Teischinger

Professor
Institute of Wood Science and Technology
University of Renewable Resources and Applied Life Sciences
Gregor Mendel Strasse 33, A-1180 Vienna, Austria

## ABSTRACT

Using a new method to determine the longitudinal shear modulus (G) and shear strength ($\tau$) of solid wood in a single test, the observed shear properties of normal (NW) and compression wood (CW) of larch samples were related to their microstructure, i.e., density, microfibril angle (MFA), and lignin content. To estimate the effective G of the solid cell wall, a semi-empirical model, which calculates G on the basis of porosity by extrapolation from experimental data, was used. For comparison, the effective G was derived from an analytical model, which considers the cell wall as a unidirectional laminate consisting of fiber and matrix material. The analytical model proved that the effect of increased MFA and higher lignin content on G in CW balance each other to a large degree. The effective G of the cell wall calculated by the analytical unidirectional laminate model was close to the estimate of the effective cell wall G performed by extrapolation from experimental data. Both models and mechanical test results demonstrated that effects of variability in cell-wall ultrastructure on G are minor, compared to effects of porosity and density, respectively. A multivariate regression model combining G and density showed that a good estimate of $\tau$ can be achieved using these input data.

*Keywords:* Cellulose, compression wood, larch (*Larix decidua* Mill.), lignin, microfibril angle, Mode II, normal wood, shear modulus, shear strength.

## INTRODUCTION

The dimensions of wooden load-bearing structures are limited by stiffness and critical stress. In short, deep beams, shear strength becomes a critical factor (Keenan and Selby 1973). The design stresses for shear assigned by different standards are rather conservative (e.g., DIN 4074-1 [1989], ÖNORM B 4100-2 [1997]). This conservatism is partly due to the particular characteristics of shear failure, which occurs abruptly. The fact that shear strength ($\tau$) is difficult to predict from parameters recorded in nondestructive testing also contributes to this cautiousness.

Different standardized and non-standardized methods for the determination of the shear properties of wood and wood products exist (ASTM D-143 [1992a], D-3044 [1992b], DIN 52187 [1979], EN 408 [1999]; Biblis and Fitzgerald 1970; Liu 1984; Zhang and Sliker 1991; Janowiak

and Pellerin 1991; Lang 1997; Divos et al. 1998), but only a few methods allow the determination of $\tau$ and the shear modulus (G) in a single test (ASTM D1037 [1992c]; EN 789 [2002]; Bateman et al. 1990; Zhang and Sliker 1991; Szalai 1992). Zhang and Sliker (1991) and Szalai (1992) proposed a method for the determination of G and $\tau$, deriving these values from off-axis tensile and compression tests. Bateman et al. (1990) used a five-point bending test for the determination of interlaminar shear properties, but the shear strength was found to be a function of the span-to-depth ratio of the beam. The EN 789 method and the ASTM D1037 interlaminar shear test of wood based panels use a specimen that is bonded between two steel plates loaded in compression. This test fixture causes the problem of bonding wood to metal surfaces. Pilot tests with solid wood based on the ASTM D1037 and EN 789 test method using different types of adhesives revealed a maximum achievable glueline shear strength of 9 MPa. Considering the fact that the longitudinal shear strength of many softwood species reaches a similar level (Forest Products Laboratory 1999), this method seems inappropriate for shear-testing of solid wood because of the limited shear strength at the wood-metal interface. To overcome the problem of wood-metal bonding, a modified edgewise shear test set-up similar to ASTM D 1037 was designed (see Fig. 1).

The mechanical properties of wood are determined by the structure of the cells and of the cell walls (Côté 1981). The cell-wall properties depend on ultrastructure and on the properties of the wood polymers. Bergander and Salmén (2002) investigated the influence of the elastic constants of the three wood polymers cellulose, hemicellulose, and lignin, the microfibril angle (MFA), and the thickness of the middle secondary cell-wall layer ($S_2$) on the axial and transverse mechanical properties of wood. Their results showed a good agreement between the modeled and experimental values.

The present study focuses on the macroscopic shear properties of a softwood species and their relationship with microstructure. In order to obtain specimens with maximum microstructural variability and different mechanical behavior,
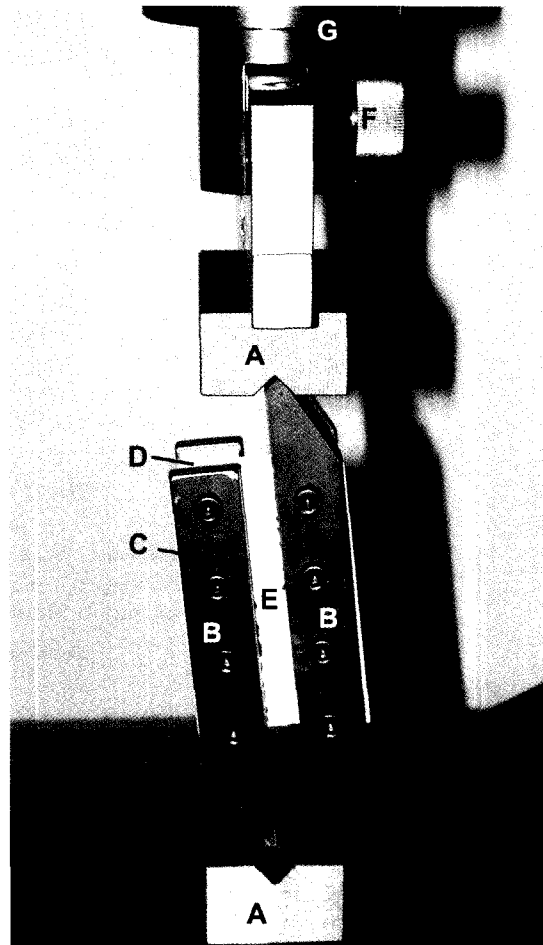


FIG. 1. (A) upper and lower fitting, (B) loading rails, (C) glueline between support blocks (D) and sample (E), (F) bolt bearing, (G) loading head. Total length of the shear mounting = 180 mm, length of the loading rails = 150 mm, slope of the shear mounting = 5°, and shear sample dimensions as follows: length × width × thickness = 100 × 14 × 14 mm.

normal wood (NW) and compression wood (CW) were used for mechanical tests. Density, MFA, and lignin content will be considered to provide a better understanding of the shear behavior of solid wood.

## MATERIAL AND METHODS

### Experimental procedure

Two boards of NW and CW of a larch tree (*Larix decidua* Mill.) were selected for this study. The annual growth rings of the NW were narrow

(mean ring width = 1.4 mm) and the latewood percentage amounted to 35% (latewood width divided by total ring width). The CW board consisted of wide annual rings (3.0 mm) with a maximum compression wood percentage of 55%. The two boards were sawn into laths with a perfectly axial orientation, in a manner such that the sides of the laths were parallel to the growth rings and the wood rays, respectively. 24 NW and CW shear samples (14 × 14 × 100 mm) were sawn off the laths. According to the terminology of fracture description proposed by Bodig and Jayne (1982), specimens for Mode II experiments in the tangential—longitudinal (TL, 12 NW + 12 CW samples) and radial—longitudinal (RL, 12 NW + 12 CW samples) directions were prepared. For example, the notation TL indicates that the sample is loaded in longitudinal shear mode with the crack plane normal to the T direction and the crack front propagating in the L direction. The samples were stored at 20°C and 65% relative humidity for one month to ensure uniform moisture content (MC). After the mechanical tests, the MC of selected samples was determined by the oven-drying method. The oven-dry density of the shear samples was calculated from the weight and the volume, resulting in 721 ± 32 kg/m³ for CW and 589 ± 14 kg/m³ for NW, respectively.

The test fixture and the specimens used for determining G and τ are shown in Fig. 1. The test specimens were glued between two support blocks of beech wood (25 × 25 × 100 mm). A phenolic resin with a shear strength of 17 MPa was used to avoid failure within the glueline. Beech was chosen because of its high shear modulus G = 1.60 GPa and shear strength τ = 20 MPa (Keylwerth 1951). Finally, two pairs of steel loading rails were glued to the beech support blocks by means of a rapidly hardening epoxy glue and additionally clamped with four screws.

All samples were tested in a Zwick/Roell Z100 kN universal testing machine at a crosshead speed of 0.6 mm/min. The shear deformation was computed from the crosshead movement by Eq. (1).

$$G = (F_1 - F_2) \, t / (\cos (8°) \, (u_1 - u_2) \, w \, l) \quad (1)$$

$F_1$    10% of $F_{max}$

$F_2$    50% of $F_{max}$
$u_1$    deformation at $F_1$
$u_2$    deformation at $F_2$
t    sample thickness
w    width of the sample
l    length of the sample
8°    slope of the loading rails

To correct for machine compliance, a 25-mm-thick steel plate was clamped between the two pairs of steel loading rails instead of the sample, and a load-deformation curve was recorded. This curve was superimposed on the test data to obtain true sample deformation values.

## Modeling the cell-wall shear modulus

In addition to mechanical testing, mathematical models play an important role in the understanding of the behavior of wood. To obtain an estimate of the Young's modulus for a porous material at given porosity, Kovacik (1999) suggested a semi-empirical model (Eq. 2), which was recently shown to be also valid for the prediction of the shear modulus (Kovacik 2001). In this model a specific shear modulus for the cell-wall material is estimated without any consideration of the structure, composition, and construction of the layered wood cell wall.

$$G = G_{eff} \, (p_c - p)^f / p_c \quad \text{for } p \le p_c \quad (2)$$

In Eq. (2), p is the porosity, $G_{eff}$ is the shear modulus of the solid cell-wall material, $p_c$ is a threshold value indicating the porosity at which the effective shear modulus becomes zero, and f is a characteristic exponent for the shear modulus of porous materials. The porosity of the samples was determined using Eq. (3) (Kollmann 1951) where 1.5 is the density of the solid cell wall (Kellogg et al. 1975) and $\rho_0$ the oven-dry density of the wood specimen. To evaluate $G_{eff}$ of the cell-wall material of NW and CW, G was plotted against p.

$$p = 1 - \rho_0 / 1.5 \quad (3)$$

A Levenberg–Marquardt nonlinear least squares regression was used to estimate the parameters $G_{eff}$, $p_c$, and f of Eq. (2). Thus, an inher-

ent trend in the experimental data set was extrapolated, and it was assumed that G at zero porosity represents the shear modulus of the cell wall.

In addition to this model, which estimates the shear modulus of the cell-wall material on the basis of extrapolation from experimental data, a second, analytical model delivering the cell-wall shear modulus based on orthotropic elasticity was calculated. Considering the cell wall as a unidirectional laminate (Daniel and Ishai 1994) consisting of cellulose, hemicellulose, and lignin, its mechanical properties are influenced mainly by the mechanical properties of the fiber and matrix material, the thickness fraction of both components, and by the fiber orientation. Table 1 shows elastic constants of the three wood components as compiled by Bergander and Salmén (2000, 2002). The cell-wall model used for the calculation is composed of five layers, i.e., middle lamella (ML), primary cell-wall (PW), and the outer, middle, and inner secondary wall ($S_1$, $S_2$, $S_3$). The average orientation of the microfibrils of each layer and its relative composition by mass of the three wood components lignin (L), hemicellulose (HC), and cellulose (C) are given in Table 2, taken from Panshin and DeZeeuw (1970). Thickness fractions of each layer were obtained from a typical earlywood and latewood fiber of a softwood (Fengel and Stoll 1973; Fengel and Wegener 1984). To get an estimate of the shear modulus of the whole tissue, the particular fiber to be modeled is a mixture of an earlywood and latewood fiber with a weighting factor corresponding to the actual latewood proportion of the NW samples (thickness fractions, see Table 2). Table 3 shows thickness fraction and composition of the different layers of CW according to its ultrastructure (Timell 1985). With the exception of the microfibril orientation within the $S_2$ layer, data from Table 2 and Table 3 were taken to

TABLE 2.  *Fibril orientation ($\theta$) and thickness fraction (t) of each cell-wall layer and its relative composition by mass of cellulose (C), hemicellulose (HC), and lignin (L) of normal wood.*

| layer | t (%) | $\theta$ (°) | C (%) | HC (%) | L (%) |
|---|---|---|---|---|---|
| ML | 10 | random | 8 | 36 | 56 |
| PW | 2 | random | 15 | 32 | 53 |
| $S_1$ | 7 | ±70 | 28 | 31 | 41 |
| $S_2$ | 80 | 13.5 | 50 | 31 | 19 |
| $S_3$ | 1 | 70 | 48 | 36 | 16 |

model the shear modulus of the NW and CW cell wall. To investigate the effect of the microfibil orientation within the thickest and most important cell-wall layer $S_2$, this orientation was varied between 0° and 45° in the model of normal wood and slight and severe compression wood, respectively, which corresponds to the possible maximum variability of MFA in the $S_2$ of softwood reported in the literature (Bergander and Salmén 2002; Lichtenegger et al. 1999; Donaldson 1991 and 1992). To get input data for the NW and CW of European larch used in our experiments, the microfibril orientation and the lignin content of $S_2$ were determined.

For MFA determination, microsections were prepared from NW and CW. The MFA of the different tissues, i.e., earlywood, latewood, and compression wood was determined by iodine-potassium staining. A detailed description of this method is given in Bailey and Vestal (1937) and Huang et al. (1997). The lignin content of NW and CW $S_2$ cell-wall layers was measured by UV-microscopy (Scott et al. 1969). Growth rings of NW and CW containing both earlywood and latewood were dehydrated in alcohol and ace-

TABLE 1.    *Elastic constants for the cell-wall polymers cellulose (C), hemicellulose (HC), and lignin (L).*

|  | C (GPa) | HC (GPa) | L (GPa) |
|---|---|---|---|
| $E_1$ | 167.5 | 7.0 | 2.0 |
| $E_2$ | 30.5 | 3.5 | 2.0 |
| $G_{12}$ | 3.0 | 1.8 | 0.8 |

TABLE 3. *Fibril orientation ($\theta$) and thickness fraction (t) of each cell-wall layer and its relative composition by mass of cellulose (C), hemicellulose (HC), and lignin (L) of slight (*) and severe (**) compression wood.*

| layer | t (%) | $\theta$ (°) | C (%) | HC (%) | L (%) |
|---|---|---|---|---|---|
| ML | 2 | random | 14 | 36 | 50 |
| PW | 4 | random | 18 | 32 | 50 |
| $S_1$ | 28 | ±80*/±85** | 28 | 31 | 41 |
| $S_2$ | 66 | - | 40* / 30** | 30 | 30* / 40** |

tone and embedded in epoxy resin. Then, 1-μm-thick cross sections were prepared by means of a Leica Ultracut ultramicrotome. In a Zeiss MPM 800 spectrophotometermicroscope, the UV-absorbance at a wavelength of 280 nm was recorded in the $S_2$ using a measuring spot size of 1 μm. Lignin content was calculated from the absorbance values according to Scott et al. (1969).

Using the input data obtained as described above, the construction of the model proceeded as follows: First, the elastic constants ($E_1$, $E_2$, $G_{12}$, $\nu_{12}$, $\nu_{21}$) for cell-wall layers of different chemical composition were calculated according to the Halpin-Tsai equations or rules of mixture (Halpin and Kardos 1976), assuming that the polymers were perfectly bonded together and underwent the same deformation under a given load. In the second step, the shear modulus of the individual composite cell-wall layers was calculated as a function of MFA (θ) as described in Eq. (4) (Daniel and Ishai 1994).

$$G_{xy}=G_{eff}=(4*(1+\nu_{12})*\cos^2\theta*\sin^2\theta/E_1+$$
$$4*(1+\nu_{21})*\cos^2\theta*\sin^2\theta/E_2+$$
$$(\cos^2\theta-\sin^2\theta)^2/G_{12})^{-1} \qquad (4)$$

Finally, the individual cell-wall layers were joined together, again according to the rules of mixture. For in-plane shear, it was assumed that the layers underwent the same shear strain at a given stress, whereas same stress at a given deformation was assumed for out-of-plane shear.

## RESULTS

### Mechanical testing

Results of mechanical tests in TR and TL mode are displayed in Fig. 2 and Fig. 3. With the exception of the shear modulus of NW, no statistically significant differences (p < 0.05) of τ and G between the two modes were observed. Therefore, no distinction between the two testing modes was made in the further analysis of the data. CW samples (τ = 11.7 ± 2.4 MPa) showed a 77% higher maximum shear strength than NW samples (τ = 6.6 ± 1.6 MPa), and the shear modulus of CW (1022 ± 172 MPa) was 48% higher than of NW (693 ± 123 MPa). Considering all



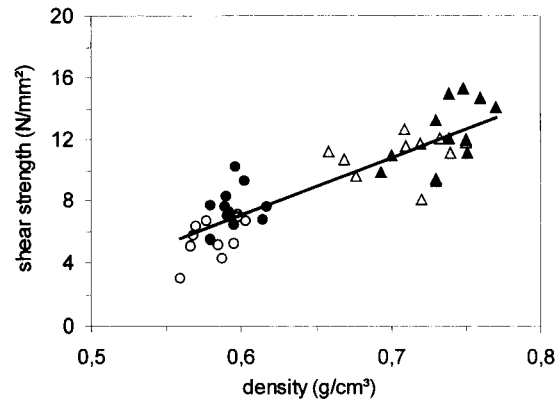FIG. 2. Shear strength plotted against density of ○ $NW_{RL}$, ● $NW_{TL}$, △ $CW_{RL}$, and ▲ $CW_{TL}$. 76 % of the variability of the shear strength can be explained by density.

NW and CW samples, a trend of increasing G with increasing density is seen. When τ is plotted against G (Fig. 4), a highly significant linear relationship is obtained. 73% of the variability of τ can be explained by G. The addition of density as a second independent variable in the regression analysis results in an increase of the explained variability of τ to 83%.

### Modeling of the cell-wall shear modulus

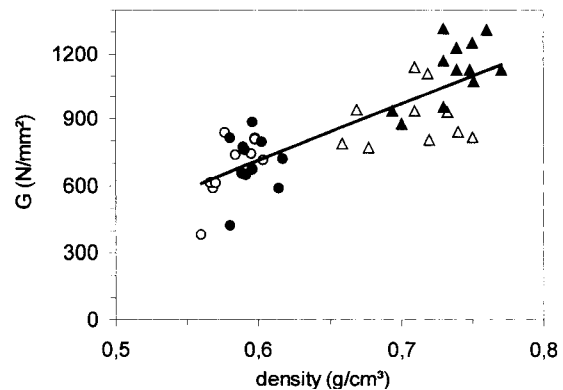Figure 5 shows the mean values of G of CW and NW tested in TR and TL modes, respec-



FIG. 3. Shear modulus plotted over density of ○ $NW_{RL}$, ● $NW_{TL}$, △ $CW_{RL}$ and, ▲ $CW_{TL}$. 67% of the variability of the shear modulus can be explained by density.
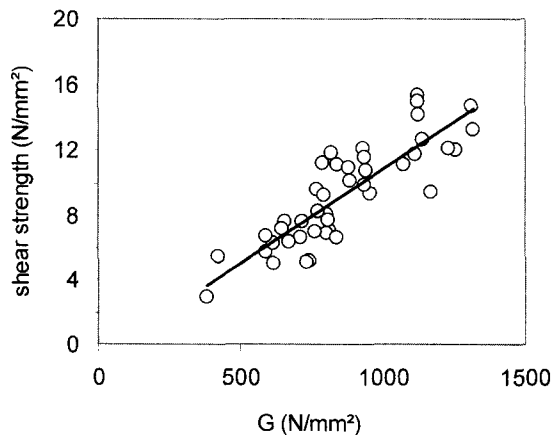
FIG. 4.   The relationship between the shear strength and the shear modulus of larch samples. 73% of the variability of the shear strength can be explained by the shear modulus.
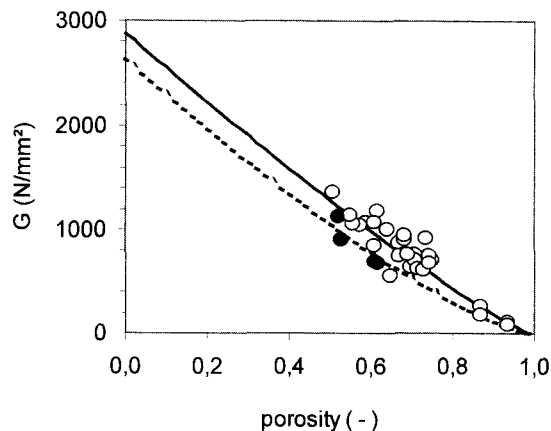


FIG. 5.   Determination of the effective shear modulus of the cell-wall of larch specimens (black circles, dotted line) and different hard- and softwoods (empty circles, continuous line) by extrapolation from experimental data using Eq. (2).

tively, plotted over porosity. Fitting Eq. (2) to G and porosity of all examined specimens, a theoretical $G_{eff}$ of the solid cell wall of 2.64 GPa is obtained ($R^2$ of the fit is 0.56). To provide additional evidence for the magnitude of $G_{eff}$ of the wood cell wall, data on shear moduli of different hardwood and softwood species were compiled from the literature (Keylwerth 1951; Zhang and Sliker 1991; Divos et al. 1998; Liu 2000) and plotted against porosity (Fig. 5). Fitting again Eq. (2) to the data, a value of 2.88 GPa is obtained for the theoretical $G_{eff}$ of the solid cell-wall ($R^2$ of the fit is 0.74).

The determination of MFA and lignin content of NW and CW showed characteristic differences as already known from the literature. The average $S_2$ MFA of the NW samples was 18° in earlywood and 5° in latewood. Using the latewood percentage of approximately 35% as a weighting factor, a mean MFA of 13.5° for NW is estimated. In CW, an average MFA of 31° was observed in both earlywood and latewood. The $S_2$ lignin content as determined by UV-microscopy varied from 20.2 ± 1.1% for NW to 33.9 ± 4.4% for CW samples.

Figure 6 shows the results of the analytical modeling of G performed on the basis of the elastic constants of cellulose, hemicellulose, and lignin. The plot of G of a cell wall containing 19% lignin in the $S_2$ against the S2 cellulose microfibril

angle demonstrates that, at an MFA of 45°, G can theoretically rise more than twice the value at an MFA of 0°. On the other hand, a higher lignin concentration, as found in compression wood, considerably reduces the effect of changing MFA. Using the results of the MFA and lignin content measurements performed on the NW and CW specimens tested in the present study, a theoretical effective shear modulus of the solid cell wall ($G_{eff}$) of 3.15 GPa for NW and 4.08 GPa for CW, respectively, is obtained (Fig. 6).

## DISCUSSION

In comparison to the published average values for the shear strength of larch wood parallel to the grain of 9.4 to 9.9 MPa (ÖNORM B 3012 [1997]; Sell 1989; Forest Products Laboratory 1999), the shear strength of 6.6 MPa measured for larch NW tested in this study is relatively low. The reason for this difference may be found in the different test configurations used. ASTM D 143 and DIN 52187 are block shear tests. In this test configuration, pure shear stress does not exist (Liu 1984). Additionally, these standardized tests are biased by considerable stresses normal to the shear crack plane (Liu 1984; Lang 1997; Liu 2000). When an optimized test geometry with minimized normal stress occurrence